

Absence of spin-boson quantum phase transition for transmon qubits

Kuljeet Kaur,¹ Théo Sépulcre,² Nicolas Roch,² Izak Snyman,³ Serge Florens,² and Soumya Bera¹

¹*Department of Physics, Indian Institute of Technology Bombay, Mumbai 400076, India*

²*Univ. Grenoble Alpes, CNRS, Institut Néel, F-38000 Grenoble, France*

³*Mandelstam Institute for Theoretical Physics, School of Physics, University of the Witwatersrand, Johannesburg, South Africa*

Superconducting circuits are currently developed as a versatile platform for the exploration of many-body physics, both at the analog and digital levels. Their building blocks are often idealized as two-level qubits, drawing powerful analogies to quantum spin models. For a charge qubit that is capacitively coupled to a transmission line, this analogy leads to the celebrated spin-boson description of quantum dissipation. We put here into evidence a failure of the two-level paradigm for realistic superconducting devices, due to electrostatic constraints which limit the maximum strength of dissipation. These prevent the occurrence of the spin-boson quantum phase transition for transmons, even up to relatively large non-linearities. A different picture for the many-body ground state describing strongly dissipative transmons is proposed, showing unusual zero point fluctuations.

Quantum computation has been hailed as a promising avenue to tackle a large class of unsolved problems, from physics and chemistry [1] to algorithmic complexity [2], following an original proposition from Feynman [3], long before the technological and conceptual tools were developed to make such ideas tangible. While a general purpose digital quantum computer could theoretically outperform classical hardware for some exponentially hard tasks, building such a complex quantum machine is at present still out of reach. For this reason, analog quantum simulation has been put forward as a crucial milestone [4], aiming at the design of fully controllable experimental devices mimicking the features of difficult quantum problems of interest. This route has met tremendous success in the past, with the realization of Kondo impurities in quantum dots [5], the simulation of artificial solids in optical lattices [6], and is gaining momentum with new tools from superconducting circuits [7–13]. Ironically, while Feynman anticipated quantum simulators [3], he often warned in his lectures (where analogy was used as a powerful teaching method) that there is no such thing as a perfect analogue, and that some interesting physics can emerge when the analogy breaks down [14]. Exploring the limitations of realistic superconducting qubits in simulating dissipative two-level systems is the main purpose of this Letter. In the process we will unveil the unique many-body physics of such simulators.

In this context, three important challenges must be addressed. First, most quantum computation/simulation protocols assume that superconducting qubits behave as idealized spin 1/2 degrees of freedom, which is clearly invalid at strong driving [15], and generally questionable in the many-body regime due to proliferation of quantum states. We will propose here a microscopic approach that takes into account the full Josephson potential of the qubit. Second, quantitative modelling of designs involving several qubits or resonators demands incorporating the full capacitance network, even in the linear regime [16–20]. We will see that such electrokinetic con-

siderations impose strong constraints on the underlying models. Third, many-body effects beyond the RWA approximation are notoriously difficult to simulate due to an exponentially large Hilbert space, for instance in the ultra-strong coupling regime of dissipation [21–23]. To overcome this challenge, we will develop new analytical and numerical techniques for the quantitative analysis of quantum circuits involving many strongly interacting degrees of freedom (including charge offsets), a problem that is raising increasing interest [9, 20, 24] due to potential applications ranging from hardware-protected qubits [25, 26] to quantum optics with metamaterials [27].

Having set the stage, we propose to examine the potential implementation of many-body physics in realistic superconducting circuits from the perspective of quantum dissipation [28, 29], stressing that our findings will apply to a wider range of simulation platforms. Precedent studies of this problem [30–35] relied on the two-level approximation, which is only valid for strong non-linearities, a regime that is very hard to investigate experimentally, due to high sensitivity to external noise sources. We study the circuit of Fig. 1, composed of a superconducting qubit containing a junction with Josephson energy E_J and capacitance $C_J = C_s + C_g$ where C_s is a shunt capacitance and C_g is a gate capacitance, that is capacitively coupled via C_c to a transmission line characterized by lumped element inductance L and capacitance C . (The transmission line may be designed from an array of linear Josephson elements [20]). All nodes are grounded *via* capacitances C_g . A DC charge offset controlled by voltage V_g is included on qubit node 0, appearing as dimensionless charge $n_g = V_g C_g / 2e$. The circuit Lagrangian reads [36] (working in units of $\hbar = 2e = 1$):

$$\mathcal{L} = \frac{1}{2} \dot{\vec{\Phi}}^\top \mathbf{C} \dot{\vec{\Phi}} - \frac{1}{2} \dot{\vec{\Phi}}^\top \mathbf{1}/L \dot{\vec{\Phi}} + E_J \cos(\Phi_0) - n_g \dot{\Phi}_0, \quad (1)$$

where $\vec{\Phi} = (\Phi_0, \Phi_1, \dots)$ is a vector of dimensionless node fluxes labeled according to Fig. 1. \mathbf{C} and $\mathbf{1}/L$ are the capacitance and inductance matrices read from Fig 1, that

define a generalized eigenvalue problem $1/LP = CP\omega^2$, ω being the diagonal matrix of the system eigenfrequencies. Noting that $[P^T CP, \omega^2] = 0$, implying that we can take $P^T CP$ diagonal, we normalize the columns of P such that $P^T CP = \mathbb{1}$. In the new basis $\vec{\phi} = P^{-1}\vec{\Phi}$, the Lagrangian is in normal modes form:

$$\mathcal{L} = \frac{1}{2}\vec{\phi}^T(-\partial_t^2 - \omega^2)\vec{\phi} + E_J \cos\left(\sum_k P_{0k}\phi_k\right) - n_g \sum_k P_{0k}\dot{\phi}_k, \quad (2)$$

where the dispersion relation ω_k and the coupling P_{0k} are given in Supplementary Materials. The qubit degree of freedom is recovered via the change of variables:

$$\begin{cases} \varphi = \sum_k P_{0k}\phi_k \\ \varphi_m = \phi_m \end{cases}, \begin{cases} n = N_0/P_{00} \\ n_m = N_m - (P_{0m}/P_{00})N_0 \end{cases}, \quad (3)$$

where \vec{n} (resp. \vec{N}) is the vector of charges conjugate to $\vec{\varphi}$ (resp. $\vec{\phi}$). Since $\omega_0 = 0$, the change of variables does not generate any diamagnetic (or ‘ A^2 ’) term [17, 18].

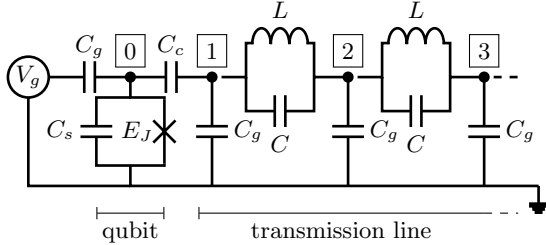


FIG. 1. Microscopic electrokinetic model for a realistic circuit of dissipative superconducting transmon. The qubit, located at node 0, is characterized by Josephson energy E_J , shunt capacitance C_s , and is capacitively coupled via C_c to a transmission line. All nodes are shunted to the ground via the capacitance C_g , and each lumped element in the line is characterized by its inductance L and self-capacitance C . Charge offsets are modeled by a DC voltage source V_g .

Once quantized in terms of creation/annihilation operators, we obtain the Hamiltonian :

$$\hat{H} = \sum_k \omega_k \hat{a}_k^\dagger \hat{a}_k + (\hat{n} - n_g) \sum_k ig_k (\hat{a}_k^\dagger - \hat{a}_k) + 4E_c (\hat{n} - n_g)^2 - E_J \cos \hat{\varphi}, \quad (4)$$

which we nickname the ‘‘transmon-boson model’’, as it generalizes the ubiquitous spin-boson model describing quantum dissipation [28, 29]. Here $g_k = \sqrt{\omega_k/2P_{0k}}$ are the couplings to the bosonic normal modes, and the qubit charging energy reads:

$$4E_c = \frac{P_{00}^2}{2} + \sum_{k \neq 0} \frac{g_k^2}{\omega_k} = \frac{P_{00}^2}{2} + \frac{1}{\pi} \int_0^\infty d\omega \frac{J(\omega)}{\omega}, \quad (5)$$

where the spectral function $J(\omega) = \pi \sum_k g_k^2 \delta(\omega_k - \omega)$ lumps together the distribution of the couplings to each mode into a single function (that is smooth for an infinite

chain) [28, 29]. It is crucial to note that the spectral function $J(\omega)$ and the charging energy E_c are not mutually independent. For the circuit of Fig. 1, we find $J(\omega) = 2\pi\alpha\omega\sqrt{1 - \omega^2/\omega_P^2}/(1 + \omega^2/\omega_J^2)\theta(\omega_P - \omega)$, dissipation strength $\alpha = (1/2\pi)[C_c/(C_c + C_J)]^2\sqrt{L/C_g}$, (angular) plasma frequency of the line $\omega_P = 1/\sqrt{L(C + C_g/4)}$, and RC cutoff of the junction $\omega_J = 1/\sqrt{LC_{\text{eff}}}$ (a derivation of these parameters is given in the Supplementary Materials). For realistic parameters describing the circuit of Fig. 1, the linear behavior of $J(\omega)$ is cut-off at a scale ω_J well below the plasma scale ω_P , thus limiting the ohmic range of dissipation.

Due to the mutual dependence between E_c and $J(\omega)$ arising from electrostatics, the dissipation strength α has an upper bound of order $E_c/\text{Min}(\omega_P, |\omega_J|)$. To show this, we parametrize the spectral function as $J(\omega) = 2\pi\alpha\omega \exp(-\omega/\omega_c)$, without specifying the origin of the cutoff ω_c . Eq. (5) gives $\alpha = [2E_c - 1/(4C_J + 4C_c)]/\omega_c$. Using E_c and ω_c as independent parameters imposes:

$$\alpha \leq \alpha_{\text{max}} = 2E_c/\omega_c. \quad (6)$$

Such electrostatic constraint must be fulfilled for any microscopic model, and in the Supplementary Materials, we provide a similar bound for the circuit of Fig. 1, showing that only the prefactor depends on the shape of the cutoff function. Clearly, the maximum value of dissipation α_{max} is attained for $C_c \rightarrow \infty$, namely when the qubit becomes wire coupled to the transmission line (see Fig. 1). The simple constraint (6) has profound consequences for the dissipative quantum mechanics of realistic superconducting qubits. Indeed, reaching the ultrastrong coupling regime ($\alpha \simeq 1$) where many-body effects are most prominent implies $E_c \simeq \omega_c$. For Cooper pair boxes (CPB) with $E_J \ll E_c$, one obtains $E_J \ll \omega_c$, and ohmic dissipation dominates the qubit dynamics, since the first transition at energy E_J is well within the linear regime of $J(\omega)$. However, for transmons with $E_J \gg E_c$, the first transition located at $\sqrt{8E_c E_J} \gg \omega_c$ now lies in the tails of the cutoff function $J(\omega)$. Hence *ultra-strong coupling physics and the spin-boson quantum phase transition* [28] are not possible for a capacitively coupled transmon qubit, shedding light on previous experimental attempts [20, 24], and extending also predictions for simpler systems of transmons coupled to single cavities [37, 38]. One can thus wonder at which range of non-linearity the two-level picture breaks down, and what kind of physical states are relevant for realistic dissipative qubits.

These questions can only be settled by reliable quantum many-body simulations of the transmon-boson Hamiltonian (4). Taking advantage of the impurity structure of the problem, we have extended the Numerical Renormalization Group (NRG) [39] to dissipative Josephson junctions, in contrast to previous approaches based on the spin-boson model and the two-level system approximation [40]. The main ingredient of NRG

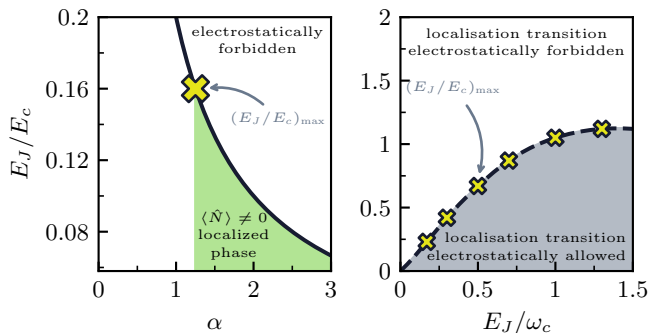


FIG. 2. Left panel: spin boson phase diagram determined from the order parameter $\langle \hat{N} \rangle$, for fixed $E_J = 0.1\omega_c$ and at the degeneracy point $n_g = 0.5$. Symmetry breaking occurs here only for ultra-strong dissipation $\alpha \gtrsim 1$ and large charging energy $E_J/E_c \ll 1$. Right panel: general phase diagram for arbitrary E_J/E_c and E_J/ω_c , ruling out a spin-boson quantum phase transition in the extended transmon regime $E_J/E_c \gtrsim 1$.

is a logarithmic discretization of the bosonic bath $J(\omega)$, with a sequence of discrete decreasing frequencies ω_k such that $\omega_{k+1} = \omega_k/\Lambda$, with $\Lambda = 2$ the Wilson parameter. The method is based on an iterative diagonalization, adding modes one by one, with a truncation of the Hilbert space at each NRG step. For the transmon-boson model (4), the first stage of the NRG starts with the junction degree of freedom, expressed in the charge basis, with up to 10^3 charge states to ensure proper convergence for all considered E_J/E_c values. The Josephson tunneling term is represented in the charge basis as $\cos(\hat{\varphi}) = 1/2 \sum_n (|n\rangle\langle n+1| + \text{h.c.})$. Typically, at each NRG step, we consider up to 10 bosonic excitations in the added environmental mode \hat{a}_k^\dagger at the discrete frequency ω_k , and we keep 250 states after truncation. We work with the Ohmic model $J(\omega) = 2\pi\alpha\omega \exp(-\omega/\omega_c)$ in units of $\omega_c = 1$, and start the NRG procedure with frequencies of order $10\omega_c$ down to the minimal frequency $10^{-14}\omega_c$ that guarantees convergence of the NRG to the full many-body ground state in the thermodynamic limit.

Our first important finding concerns the dissipation-induced spontaneous breaking of the \mathbb{Z}_2 symmetry $(|n\rangle, a_k^\dagger) \rightarrow (|2[n_g]+1-n\rangle, -a_k^\dagger)$, where $[n_g]$ is the integer part of n_g , which leaves Hamiltonian (4) invariant for $n_g = 1/2 + \text{integer}$. This spin-boson quantum phase transition is thus associated to a non-zero charge-localization order parameter $\hat{N} = \sum_n (n - n_g)|n\rangle\langle n|$. Figure 2 shows that the ground state order parameter $\langle \hat{N} \rangle$ stays zero for transmon qubits up to the maximum value of dissipation allowed by electrostatics, while the true CPB does reach a localization transition for $E_c \gg E_J$, as expected from the known physics of dissipative two-level systems. The two-level paradigm thus does not apply for transmons or even for superconducting qubits with strong non-linearities ($E_J \gtrsim E_c$), that are as close to the CPB limit as one can realistically go, before being

overwhelmed by charge noise. In order to uncover why the physics is so different in the two regimes, we now examine how one crosses over from the dissipative CPB (spin-boson model) to the dissipative transmon.

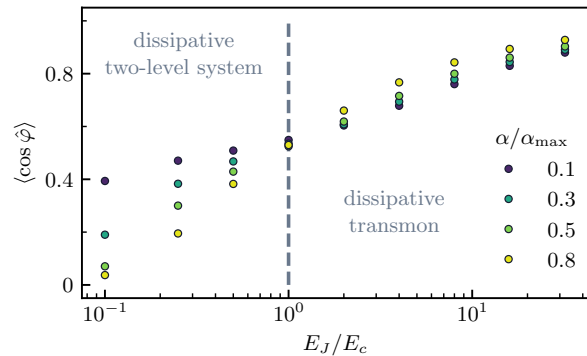


FIG. 3. NRG results for the Josephson tunneling $\langle \cos(\hat{\varphi}) \rangle$, which controls the many-body zero point fluctuations, as a function of E_J/E_c , for offset charge $n_g = 1/2$ and several values of the normalized dissipation strength α/α_{\max} . Dissipation tends to localize the phase for transmons, namely $\langle \cos(\hat{\varphi}) \rangle$ increases with α for $E_J > E_c$, in contrast to the CPB regime, where phase delocalization occurs. A surprising crossover regime with dissipation-insensitive zero point fluctuations is observed for $E_J \simeq E_c$.

Diagnosis for novel properties of dissipative transmons is given by the zero point fluctuations of the superconducting phase set by the average tunnelling $\langle \cos(\hat{\varphi}) \rangle$ in the many-body ground state. For deep transmons, $E_J \gg E_c$, $\langle \cos(\hat{\varphi}) \rangle$ increases with dissipation α , because the phase is damped by its environment towards the minimum $\hat{\varphi} = 0$ of the Josephson potential (this behavior is not captured by a two-level approximation, see Supplementary Materials). In contrast, for a CPB, $E_c \gg E_J$ and $n_g = 1/2$, the quantity $\langle \cos(\hat{\varphi}) \rangle$ decreases with dissipation since charge tends to freeze (due to Heisenberg principle, the phase delocalizes). Both behaviors are clearly evidenced in Fig 3, which shows $\langle \cos(\hat{\varphi}) \rangle$ against E_J/E_c , for several values of the normalized dissipation strength α/α_{\max} at $n_g = 0.5$. As expected from the phase diagram of Fig. 2, a crossover takes place around $E_J/E_c = 1$, between an anharmonic oscillator regime at high E_J/E_c where the phase fluctuations are damped, and a spin-boson regime where the phase fluctuations are akin to the CPB regime. Remarkably, *the crossover is characterized by quantum fluctuations of the superconducting phase that are nearly dissipation-insensitive* as seen by the narrowing spread of the points at $E_J = E_c$. This striking behavior is a manifestation of the frustrated nature of the qubit pointer states, that are neither purely phase-like nor purely charge-like in the crossover from transmons to CPB. While dissipative CPBs are well-understood physically within polaronic theory [41, 42], a new physical picture must be found to explain why the physics of dissipative transmons is so radically different.

In the deep transmon regime ($E_J \gg E_c$), phase fluctu-

ations are mostly confined at the bottom of the Josephson potential, since $\langle \cos(\hat{\varphi}) \rangle$ stays close to unity in Fig. 3. A standard approach, the self-consistent harmonic approximation (SCHA) [12, 43, 44], amounts to replacing the cosine potential in (4) by a renormalized harmonic term:

$$\hat{H}_{\text{SCHA}} = \sum_k \omega_k \hat{a}_k^\dagger \hat{a}_k + \hat{n} \sum_k i g_k (\hat{a}_k^\dagger - \hat{a}_k) + 4E_c \hat{n}^2 + \frac{E_J^*}{2} \hat{\varphi}^2 \quad (7)$$

which is nothing but the *Caldera-Leggett* model of a damped harmonic oscillator with renormalized Josephson energy E_J^* . The gate charge n_g has been removed by a gauge transform since the compactness of the phase can be neglected in this limit. However, the SCHA misses quantum phase slips associated to windings of φ by multiples of 2π , which become more and more probable for increasing values of E_c/E_J , and are highly sensitive to charge offsets due to Aharonov-Casher interference [45]. Our strategy is to deal with the charge-sensitive (or phase-compact) Hamiltonian (4) with a new class of many-body ground states chosen to keep track of the boundary conditions over the circle. We start by putting the linear parent Hamiltonian (7) into normal mode form: $\hat{H}_{\text{SCHA}} = \sum_\mu \Omega_\mu (\hat{b}_\mu^\dagger \hat{b}_\mu + 1/2)$, where Ω_μ are the eigenfrequencies of the quadratic system, and \hat{b}_μ^\dagger its raising operators (see Supplementary Materials). Charge and phase operators are expressed over the eigenmodes of the linear Hamiltonian as $\hat{n} = i \sum_\mu v_\mu (\hat{b}_\mu^\dagger - \hat{b}_\mu)$ and $\hat{\varphi} = \sum_\mu u_\mu (\hat{b}_\mu^\dagger + \hat{b}_\mu)$. Phase compactness is simply restored by displacing the superconducting phase in the vacuum of \hat{H}_{SCHA} (denoted $|0\rangle_{\text{SCHA}}$) by 2π times a winding number w , and summing over w :

$$|0_\odot\rangle = \sum_{w \in \mathbb{Z}} e^{i2\pi w \hat{n}} |0\rangle_{\text{SCHA}}. \quad (8)$$

Similar procedures have already been used to estimate fluxonium charge noise [46] and to study bulk compact-QED [47], without recourse however to a renormalized Hamiltonian (7) involving an effective Josephson energy E_J^* , which is a crucial element to capture quantitatively the physics in the crossover regime where $E_c \simeq E_J$.

The charge offset n_g seemingly drops from Hamiltonian (4) by a gauge transform $\hat{U} = \exp(in_g \hat{\varphi})$. For the linearized system, this simply adds a global phase to the harmonic state $|0\rangle_{\text{SCHA}} \rightarrow \exp(-in_g \hat{\varphi}) |0\rangle_{\text{SCHA}}$. After compactifying (8), this global phase will have a concrete effect on the observables, contrarily to the SCHA method. Using E_J^* as variational parameter, we estimate the ground state energy of \hat{H} by minimizing

$$\frac{\langle 0_\odot | \hat{H} | 0_\odot \rangle}{\langle 0_\odot | 0_\odot \rangle} = \frac{1}{2} \left(\sum_\mu \Omega_\mu - E_J u^2 \right) - \frac{E_J}{\langle 0_\odot | 0_\odot \rangle} \sum_{w \in \mathbb{Z}} \left[\frac{(\pi w)^2}{2} + (-1)^w e^{-\frac{u^2}{2}} \right] e^{-2(\pi w)^2 v^2 - i2\pi w n_g}, \quad (9)$$

where the parameters $u^2 \equiv \sum_\mu u_\mu^2$, $v^2 \equiv \sum_\mu v_\mu^2$ carry the implicit E_J^* dependence through the diagonalization of \hat{H}_{SCHA} . The offset charge n_g manifests as an Aharonov-Casher phase that depends on the winding number, thus correcting the main drawback of the SCHA, which corresponds to the term $w = 0$ only. Indeed v^2 weights the exponential corrections to the linear approximation due to phase slips, and vanishes in the limit $E_J \rightarrow \infty$, while u^2 renormalizes the Josephson energy. It is remarkable that the bosonic bath affects phase fluctuations through two scalars only, independent of the number of modes and the form of their dispersion relation.

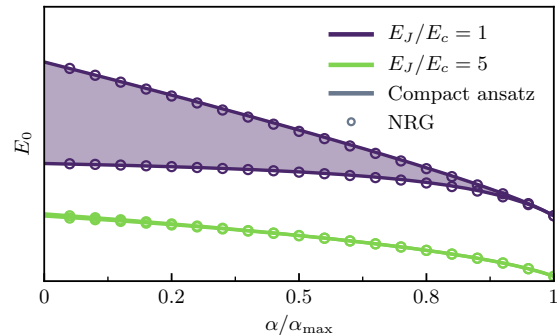


FIG. 4. Ground state energy bands associated to the offset charge n_g , both for the transmon regime (narrower band at the bottom, at $E_J/E_c = 5$) and the crossover regime (broadened band at the top, at $E_J/E_c = 1$). The analytical expression (9) from the compact Ansatz (lines) compares quantitatively to the full NRG simulation (dots).

As n_g is varied from zero to half a Cooper pair, i.e. $n_g \in [0, 1/2]$, the ground state energy sweeps out a band. Fig 4 shows this band, as calculated using the compact Ansatz as well as using NRG. The compact ansatz is quantitatively accurate for the dissipative transmon, which could have been anticipated, as it includes the main physical elements of the problem. Remarkably, it still performs very well up to the crossover to CPB, $E_c \simeq E_J$, as seen from the broad upper band in Fig. 4. This comparison establishes that phase-compact Gaussian states constitute the backbone structure of charge-sensitive superconducting devices, and opens the way to new tools for describing realistic circuits. We emphasize that approximations such as the SCHA that neglect the compactness of φ , produce a zero bandwidth.

In conclusion, we have demonstrated that realistic superconducting qubits do not show the same dissipative properties as obtained from models based on the ubiquitous two-level description. We also provided a new physical picture of the many-body wavefunction for dissipative transmons, which is described by a phase-compact Gaussian state. Reaching the spin-boson quantum phase transition requires very strong non-linearities, well beyond the transmon regime. Similar considerations could apply to a wide class of model Hamiltonians that are touted as candidates for quantum simulators [9, 12, 48].

KK and SB would like to thank IRCC, IITB for funding. SB acknowledges support from SERB-DST, India, through Ramanujan Fellowship No. SB/S2/RJN-128/2016, Early Career Research Award No. ECR/2018/000876, Matrics No. MTR/2019/000566, and MPG through the Max Planck Partner Group at IITB. SF thanks hospitality of IITB and Wits University, and acknowledges funding by PICS contract FermiCats.

-
- [1] S. McArdle, S. Endo, A. Aspuru-Guzik, S. C. Benjamin, and X. Yuan, *Rev. Mod. Phys.* **92**, 015003 (2020).
- [2] A. Montanaro, *npj Quantum Information* **2**, 15023 (2016).
- [3] R. Feynman, *Int. J. Theor. Phys.* **21**, 467 (1982).
- [4] I. M. Georgescu, S. Ashhab, and F. Nori, *Rev. Mod. Phys.* **86**, 153 (2014).
- [5] L. Kouwenhoven and L. Glazman, *Physics World* **14**, 33 (2001).
- [6] I. Bloch, J. Dalibard, and W. Zwerger, *Reviews of Modern Physics* **80**, 885 (2008).
- [7] A. A. Houck, H. E. Türeci, and J. Koch, *Nature Physics* **8**, 292 (2012).
- [8] J. Raftery, D. Sadri, S. Schmidt, H. E. Türeci, and A. A. Houck, *Physical Review X* **4**, 031043 (2014).
- [9] P. Forn-Díaz, J. J. Garcia-Ripoll, B. Peropadre, J. L. Orgiazzi, M. A. Yurtalan, R. Belyansky, C. M. Wilson, and A. Lupascu, *Nature Physics* **13**, 39 (2016).
- [10] P. Roushan et al., *Science* **358**, 1175 (2017).
- [11] R. Ma, B. Saxberg, C. Owens, N. Leung, Y. Lu, J. Simon, and D. I. Schuster, *Nature* **566**, 51 (2019).
- [12] S. Leger, J. Puertas Martinez, K. Bharadwaj, R. Dassonneville, J. Delaforce, F. Foroughi, V. Milchakov, L. Planat, O. Buisson, C. Naud, W. Hasch-Guichard, S. Florens, I. Snyman, and N. Roch, *Nature Communications* **10**, 5259 (2019).
- [13] I. Carusotto, A. A. Houck, A. J. Kollár, P. Roushan, D. I. Schuster, and J. Simon, *Nature Physics* **16**, 268 (2020).
- [14] R. P. Feynman, R. B. Leighton, and M. Sands, *The Feynman lectures on physics; New millennium ed.* (Basic Books, New York, NY, 2010).
- [15] R. Lescanne, L. Verney, Q. Ficheux, M. H. Devoret, B. Huard, M. Mirrahimi, and Z. Leghtas, *Phys. Rev. Applied* **11**, 014030 (2019).
- [16] S. E. Nigg, H. Paik, B. Vlastakis, G. Kirchmair, S. Shankar, L. Frunzio, M. H. Devoret, R. J. Schoelkopf, and S. M. Girvin, *Physical Review Letters* **108**, 260 (2012).
- [17] J. J. Garcia-Ripoll, B. Peropadre, and S. De Liberato, *Scientific Reports* **5**, srep16055 (2015).
- [18] M. Malekakhlagh, A. Petrescu, and H. E. Türeci, *Physical Review Letters* **119**, 073601 (2017).
- [19] A. Parra-Rodriguez, E. Rico, E. Solano, and I. L. Egusquiza, *Quantum Science and Technology* **3**, 024012 (2018).
- [20] J. Puertas Martinez, S. Leger, N. Gheeraert, R. Dassonneville, L. Planat, F. Foroughi, Y. Krupko, O. Buisson, C. Naud, W. Hasch-Guichard, S. Florens, I. Snyman, and N. Roch, *npj Quantum Information* **5**, 1829 (2019).
- [21] P. Forn-Díaz, L. Lamata, E. Rico, J. Kono, and E. Solano, *Reviews of Modern Physics* **91**, 025005 (2019).
- [22] A. F. Kockum, A. Miranowicz, S. De Liberato, S. Savasta, and F. Nori, *Nature Reviews Physics* **1**, 1 (2019).
- [23] A. Le Boité, *Advanced Quantum Technologies* **3**, 1900140 (2020).
- [24] R. Kuzmin, N. Mehta, N. Grabon, R. Mencia, and V. E. Manucharyan, *npj Quantum Information* **5**, 1 (2019).
- [25] D. K. Weiss, A. C. Y. Li, D. G. Ferguson, and J. Koch, *Phys Rev B* **100**, 224507 (2019).
- [26] A. Di Paolo, T. E. Baker, A. Foley, D. Sénéchal, and A. Blais, *arXiv.org* (2019), 1912.01018v1.
- [27] A. L. Grimsmo, B. Royer, J. M. Kreikebaum, Y. Ye, K. O'Brien, I. Siddiqi, and A. Blais, *arXiv.org* (2020), 2005.06483v1.
- [28] A. J. Leggett, S. Chakravarty, A. T. Dorsey, M. P. A. Fisher, A. Garg, and W. Zwerger, *Reviews of Modern Physics* **59**, 1 (1987).
- [29] U. Weiss, *Quantum Dissipative Systems* (World Scientific, 1992).
- [30] K. Le Hur, *Phys. Rev. B* **85**, 140506 (2012).
- [31] M. Goldstein, M. H. Devoret, M. Houzet, and L. I. Glazman, *Physical Review Letters* **110**, 017002 (2013).
- [32] B. Peropadre, D. Zueco, D. Porrás, and J. J. Garcia-Ripoll, *Phys. Rev. Lett.* **111**, 243602 (2013).
- [33] I. Snyman and S. Florens, *Physical Review B* **92**, 085131 (2015).
- [34] N. Gheeraert, X. H. H. Zhang, T. Sépulcre, S. Bera, N. Roch, H. U. Baranger, and S. Florens, *Physical Review A* **98**, 043816 (2018).
- [35] L. Magazzù, P. Forn-Díaz, R. Belyansky, J.-L. Orgiazzi, M. A. Yurtalan, M. R. Otto, A. Lupascu, C. M. Wilson, and M. Grifoni, *Nature Communications* **9**, 1403 (2018).
- [36] U. Vool and M. H. Devoret, *International Journal of Circuit Theory and Applications* **45**, 897 (2017).
- [37] S. J. Bosman, M. F. Gely, V. Singh, D. Bothner, A. Castellanos-Gomez, and G. A. Steele, *Phys Rev B* **95**, 224515 (2017).
- [38] T. Jaako, Z.-L. Xiang, J. J. Garcia-Ripoll, and P. Rabl, *Physical Review A* **94**, 033850 (2016).
- [39] R. Bulla, T. A. Costi, and T. Pruschke, *Rev. Mod. Phys.* **80**, 395 (2008).
- [40] R. Bulla, N.-H. Tong, and M. Vojta, *Phys. Rev. Lett.* **91**, 170601 (2003).
- [41] R. Silbey and R. A. Harris, *J. Chem. Phys.* **80**, 2615 (1984).
- [42] S. Bera, S. Florens, H. U. Baranger, N. Roch, A. Nazir, and A. W. Chin, *Physical Review B* **89**, 121108 (2014).
- [43] A. D. Zaikin and S. V. Panyukov, *JETP Lett.* **43**, 670 (1986).
- [44] T. Giamarchi, *Quantum physics in one dimension* (Oxford, 2003).
- [45] M. Bell, W. Zhang, L. Ioffe, and M. Gershenson, *Physical Review Letters* **116**, 107002 (2016).
- [46] A. Mizel and Y. Yanay, *arXiv:1910.01090 [cond-mat, physics:quant-ph]* (2019), arXiv: 1910.01090.
- [47] J. Bender, P. Emonts, E. Zohar, and J. I. Cirac, *arXiv.org* (2020), 2006.10038.
- [48] A. Murani, N. Bourlet, H. le Sueur, F. Portier, C. Altimiras, D. Esteve, H. Grabert, J. Stockburger, J. Ankerhold, and P. Joyez, *Phys. Rev. X* **10**, 021003 (2020).

Finally, we have to compute the normalization factors. First, one should note that the $k = 0$ eigenfrequency is 0. Equations (S4), (S5), (S6) do not hold in this case, such that matrix elements P_{i0} must be computed by normalization of $\mathbf{P}^\top \mathbf{C} \mathbf{P}$, which leads to $P_{00} = 1/\sqrt{C_J + C_c}$, $P_{i0} = 0 \forall i > 0$. This zero mode is then localized on the zeroth site: we recognize the transmon degree of freedom, which will be singled out in the main text by a change of variable. The other normalisation factors are computed from the following matrix elements :

$$\forall l, l' \neq 0, \quad \sum_{i,j=1}^{\infty} P_{il} C_{ij} P_{jl'} = \left(C_g \sum_{i=1}^{\infty} P_{il} P_{il'} + \frac{C_c C_J}{C_c + C_J} P_{1l} P_{1l'} \right) \left(1 + 4 \frac{C}{C_g} \sin^2(k_l/2) \right). \quad (\text{S9})$$

This matrix must be diagonal, so we collect only the terms proportional to $\delta_{l,l'}$. Expanding the first part as

$$\begin{aligned} \sum_{i=1}^{\infty} P_{il} P_{il'} &= \frac{1}{2} N_l N_{l'} \sum_{j=0}^{\infty} \cos(j(k_l + k_{l'})) \cos(\theta_l + \theta_{l'}) + \cos(j(k_l - k_{l'})) \cos(\theta_l - \theta_{l'}) \\ &\quad - \sin(j(k_l + k_{l'})) \sin(\theta_l + \theta_{l'}) + \sin(j(k_l - k_{l'})) \sin(\theta_l - \theta_{l'}). \end{aligned} \quad (\text{S10})$$

Using the identity $\lim_{n \rightarrow \infty} \sum_{j=0}^n \cos(jk_l) = 1/2 + n\delta_{l,0}$ we can deduce the normalisation factor N_l . With equation (S4), we get an analytic expression of the couplings for a large but finite number of modes N_{modes} :

$$P_{00} = \frac{1}{\sqrt{C_J + C_c}}, \quad P_{0l} = \frac{C_c}{C_J + C_c} \sqrt{\frac{2}{N_{\text{modes}}}} (C_g + 4C \sin^2(k_l/2))^{-\frac{1}{2}} \left(1 + \left(2 \frac{C_f}{C_g} - 1 \right)^2 \tan^2(k_l/2) \right)^{-\frac{1}{2}}. \quad (\text{S11})$$

These expressions match the results from the numerical diagonalization of the Lagrangian (S1) performed with a finite number N_{modes} of sites, as soon as $N_{\text{modes}} \gtrsim 10$.

Spectral function. The spectral function gives a more convenient tool to describe this system with a small number of relevant parameters. It is defined as a continuous function of frequency, $J(\omega) = \pi \sum_l g_{k_l}^2 \delta(\omega - \omega_{k_l})$. The g_k couplings are defined in the main text as $g_{k_l} = \sqrt{\omega_{k_l}/2} P_{0l}$. All the dependencies in the wave number k_l can be expressed in terms of ω_k using the dispersion relation (S7). We also change sums over modes to integrals in the limit $N_{\text{modes}} \rightarrow \infty$:

$$\frac{1}{N_{\text{modes}}} \sum_l F[k_l] \rightarrow \frac{1}{\pi} \int_0^\pi dk F[k], \quad (\text{S12})$$

$$J(\omega) = N_{\text{modes}} \frac{dk}{d\omega} [g(\omega)]^2 = \left(\frac{C_c}{C_c + C_J} \right)^2 \sqrt{\frac{L}{C_g}} \omega \frac{\sqrt{1 - \omega^2/\omega_P^2}}{1 + \omega^2 \left(1/\omega_Q^2 - 1/\omega_P^2 \right)} \theta(\omega_P - \omega), \quad (\text{S13})$$

with $\omega_P = \omega_0/\sqrt{1 + 4C/C_g}$ the plasma frequency of the chain, and $\omega_Q = \omega_P \sqrt{1 + 4C/C_g}/(2C_f/C_g - 1)$ a characteristic frequency related to the qubit. From Eq. (S13), it is clear that the denominator is never vanishing within the band $\omega \in [0, \omega_P]$ (otherwise $J(\omega)$ would be singular). Using the expression for ω_P and ω_Q , and $1/\omega_J^2 \equiv 1/\omega_Q^2 - 1/\omega_P^2$, we recover the low frequency cutoff of the transmon ω_J defined in the main text.

For small frequencies, $J(\omega)$ obeys the so-called Ohmic behavior, $J(\omega) \simeq 2\pi\alpha\omega$, which defines the coupling strength α . A higher frequencies, $J(\omega)$ quickly vanishes as $1/\omega^2$, provided $\omega_J \ll \omega_P$. Most experimental devices verify this condition. On the other hand, if $\omega_J \gg \omega_P$, $J(\omega)$ displays a square-root hard cut-off at $\omega = \omega_P$. In many cases, the exact form of the cut-off is not relevant, and we replace it by an exponential cut-off at $\omega_c = \min\{\omega_J, \omega_P\}$, $J(\omega) = 2\pi\alpha\omega \exp(-\omega/\omega_c)$, which is the spectral function used in the main text to perform the numerical computations.

Microscopic derivation of the electrostatic bound on dissipation. The charging energy of our microscopic circuit explicitly reads

$$E_c = \frac{1}{8} \left(C_J + C_c - \frac{C_c^2}{C_c + \frac{C_g}{2} + \sqrt{C_g \left(\frac{C_g}{4} + C \right)}} \right)^{-1}. \quad (\text{S14})$$

This result can be obtained by noting that $E_c = C_{00}^{-1}/8$ and analytically inverting the capacitance matrix. From equation (5) in the main text one can reach the same result, recast into

$$8E_c = \frac{1}{C_c + C_J} + 2\pi\alpha \frac{\omega_J^2}{\omega_P} \left(\sqrt{1 + \frac{\omega_P^2}{\omega_J^2}} - 1 \right) \geq 2\pi\alpha \frac{\omega_J^2}{\omega_P} \left(\sqrt{1 + \frac{\omega_P^2}{\omega_J^2}} - 1 \right), \quad (\text{S15})$$

by integrating the spectral function (S13) over ω . Thus the dissipation strength α obeys the inequality

$$\alpha \leq \frac{4E_c}{\pi\omega_P} \left(\sqrt{1 + \frac{\omega_P^2}{\omega_J^2}} + 1 \right). \quad (\text{S16})$$

When $\omega_J \ll \omega_P$ (which is the typical situation for realistic devices), the electrostatic bound $\alpha \leq 4E_c/(\pi\omega_J)$ assumes the same form as in the main text (albeit with a different numerical prefactor), while for $\omega_J \gg \omega_P$ the bound reads $\alpha \leq 8E_c/(\pi\omega_P)$.

COMPACT ANSATZ WAVEFUNCTION FOR CHARGE SENSITIVE CIRCUITS

We build in this section the compact ansatz step by step, following the outline of the main text. While our approach is completely generic to charge sensitive superconducting circuits, we focus here on the transmon-boson Hamiltonian:

$$\hat{H} = 4E_c(\hat{n} - n_g)^2 - E_J \cos \hat{\varphi} + (\hat{n} - n_g) \sum_k ig_k(\hat{a}_k^\dagger - \hat{a}_k) + \sum_k \omega_k \hat{a}_k^\dagger \hat{a}_k, \quad (\text{S17})$$

where the discrete sums over the wave vector k run on the Brillouin zone $[0, \pi]$. The renormalized linear approximation, that holds in the deep transmon regime where the phase fluctuations are much smaller than 2π , is used as a linearized parent Hamiltonian for our variational trial state. It reads:

$$\hat{H}_{\text{SCHA}} = 4E_c \hat{n}^2 + \frac{E_J^*}{2} \hat{\varphi}^2 + i\hat{n} \sum_k g_k(\hat{a}_k^\dagger - \hat{a}_k) + \sum_k \omega_k \left(\hat{a}_k^\dagger \hat{a}_k + 1/2 \right). \quad (\text{S18})$$

Here the charge offset n_g was gauged out since the phase is uncompact in the linear approximation, and E_J^* is a free parameter used in the variational method, after compactification is applied. This Hamiltonian can be brought to diagonal form by a Bogoliubov rotation mixing the transmon degree of freedom and bosons from the environment. We use greek symbols to denote jointly the transmon and bosons variables, such that $\hat{n}_\mu = (\hat{n}, \hat{n}_1, \hat{n}_2, \dots)$. Then, up to rescaling of $\hat{\varphi}$ and \hat{n} ,

$$\begin{aligned} \hat{H}_{\text{SCHA}} &= \frac{1}{2} \sum_\mu \hat{\varphi}_\mu \hat{\varphi}_\mu + \frac{1}{2} \sum_{\sigma\rho} \hat{n}_\sigma \mathbf{M}_{\sigma\rho} \hat{n}_\rho \\ &= \sum_\mu \Omega_\mu (\hat{b}_\mu^\dagger \hat{b}_\mu + \frac{1}{2}), \end{aligned} \quad \text{where } \mathbf{M} = \begin{bmatrix} \frac{8E_J E_c}{g_1 \sqrt{2E_J \omega_1}} & g_1 \sqrt{2E_J \omega_1} & g_2 \sqrt{2E_J \omega_2} & \dots \\ g_1 \sqrt{2E_J \omega_1} & \omega_1^2 & & \\ g_2 \sqrt{2E_J \omega_2} & & \omega_2^2 & \\ \vdots & & & \ddots \end{bmatrix} \quad (\text{S19})$$

with Ω_μ the eigen-frequencies of the linear system and b_μ, b_μ^\dagger its raising/lowering operators. The last equation is obtained by diagonalization of matrix \mathbf{M} , which assumes an arrowhead form; efficient numerical algorithms exist for such eigenvalue problems, as well as perturbative series expansion. We can decompose the transmon variables on this new basis. To do so, we define the coefficients u_μ and v_μ such that

$$\hat{n} = i \sum_\nu v_\nu (\hat{b}_\nu^\dagger - \hat{b}_\nu) \quad \text{and} \quad \hat{\varphi} = \sum_\nu u_\nu (\hat{b}_\nu^\dagger + \hat{b}_\nu). \quad (\text{S20})$$

We then enforce the periodic boundary conditions (compactification) by repeatedly displacing the ground state of H_{SCHA} , noted $|0\rangle$, by an integer times 2π :

$$|0_\circ\rangle = \sum_{w \in \mathbb{Z}} e^{i2\pi w \hat{n}} |0\rangle, \quad \text{where } \hat{b}_\mu |0\rangle = 0 \quad \forall \mu. \quad (\text{S21})$$

Regularisation. With such a definition, $|0_\circ\rangle$ has infinite norm, because the associated wave function is both periodic and defined over \mathbb{R} . Indeed, by re-indexing sums over winding numbers,

$$\langle 0_\circ | 0_\circ \rangle = \sum_{v, w \in \mathbb{Z}} \int_{\mathbb{R}} d\varphi \langle 0 | \varphi - 2\pi v \rangle \langle \varphi + 2\pi w | 0 \rangle = \langle 0 | 0_\circ \rangle \left(\sum_{v \in \mathbb{Z}} 1 \right), \quad (\text{S22})$$

which is clearly infinite. A way out is to restrict the wave-function over the interval $[0, 2\pi[$, which is in fact equivalent to simply drop the infinite factor in the last expression:

$$\begin{aligned} \langle 0|0_{\mathcal{O}}\rangle & \left(\sum_{v \in \mathbb{Z}} 1 \right) \xrightarrow[\text{to } [0, 2\pi[]{\text{restricted}}}{\sum_{v, w \in \mathbb{Z}} \int_0^{2\pi} d\varphi \langle 0|\varphi - 2\pi v\rangle \langle \varphi + 2\pi w|0\rangle} \\ & = \sum_{v, w \in \mathbb{Z}} \int_{2\pi v}^{2\pi(v+w)} d\varphi \langle 0|\varphi\rangle \langle \varphi + 2\pi(v+w)|0\rangle = \langle 0|0_{\mathcal{O}}\rangle. \end{aligned} \quad (\text{S23})$$

The last line is obtained with a relabeling of the sums $w' = w + v$, and patching the integrals together to get back an integral on \mathbb{R} . The same trick can be used for expectation values of any operator $\hat{\mathcal{O}}$, provided that it is itself 2π -periodic, which means that $[\hat{\mathcal{O}}, \sum_w \exp(i2\pi w \hat{n})] = 0$.

Aharonov-Casher phases. We already mentioned that n_g acts as a gauge potential on the system. It can usually be removed from the Hamiltonian by a gauge transformation $\hat{U} = \exp(in_g \hat{\varphi})$, which however affects the boundary condition on the phase (unless the model is not compact). Under such a transformation, $\hat{H}_{\text{SCHA}}(n_g) = \hat{U}^\dagger \hat{H}_{\text{SCHA}}(0) \hat{U}$. It can be checked that $\hat{U}^\dagger |0\rangle$ is an eigenstate of $\hat{H}_{\text{SCHA}}(n_g)$. For a non-compact model, the gauge has no observable effect, but the compactification process will change this state of affairs, since

$$\sum_{w \in \mathbb{Z}} e^{i2\pi w \hat{n}} \hat{U}^\dagger |0\rangle = \hat{U}^\dagger \sum_{w \in \mathbb{Z}} e^{i2\pi w (\hat{n} - n_g)} |0\rangle. \quad (\text{S24})$$

As an example, the effect on the ansatz norm is :

$$\langle 0_{\mathcal{O}}|0_{\mathcal{O}}\rangle = \sum_{v, w \in \mathbb{Z}} \langle 0|e^{-i2\pi v(\hat{n} - n_g)} \hat{U}^\dagger e^{i2\pi w(\hat{n} - n_g)} |0\rangle = \sum_{w \in \mathbb{Z}} e^{-i2\pi w n_g} \langle 0|e^{i2\pi w \hat{n}} |0\rangle, \quad (\text{S25})$$

using $\hat{U} \hat{U}^\dagger = \mathbb{1}$ and the same infinite factor canceling argument as before. The offset charge effect is seen as an Aharonov-Casher phase that depends on the winding number. The interference between different winding numbers will create an observable effect due to the gauge. The same argument can be used for the expectation value of any gauge invariant operator $\hat{\mathcal{O}}$, *i.e.* $[\hat{\mathcal{O}}, \hat{U}] = 0$.

Zero point phase fluctuations. Since $\cos \hat{\varphi}$ is both 2π -periodic and gauge invariant, its expectation value is evaluated using the two previous tricks. Then, expressing every operator in terms of $\hat{b}_\mu^\dagger, \hat{b}_\mu$ with (S20) :

$$\begin{aligned} \langle 0_{\mathcal{O}}|\cos \hat{\varphi}|0_{\mathcal{O}}\rangle & = \frac{1}{2} \sum_{\pm, w \in \mathbb{Z}} e^{-i2\pi w n_g} \langle 0|\exp\left(\pm i \sum_{\sigma} u_{\sigma} (\hat{b}_{\sigma}^{\dagger} + \hat{b}_{\sigma})\right) \exp\left(-2\pi w \sum_{\rho} v_{\rho} (\hat{b}_{\rho}^{\dagger} - \hat{b}_{\rho})\right)|0\rangle \\ & = e^{-\frac{1}{2} \sum_{\nu} (u_{\nu})^2} \sum_w (-1)^w e^{-2(\pi w)^2 \sum_{\mu} (v_{\mu})^2 - i2\pi w n_g}. \end{aligned} \quad (\text{S26})$$

Note that since the state norm isn't unity, normalization is necessary, by a factor $\langle 0_{\mathcal{O}}|0_{\mathcal{O}}\rangle = \sum_w \exp(-2(\pi w)^2 v^{\mu} v_{\mu})$. Clearly, $v^2 \equiv \sum_{\mu} (v^{\mu})^2$ weights the corrections from non-zero winding numbers. It vanishes when $E_J \rightarrow \infty$, providing a pure harmonic oscillator behavior in this limit. At finite E_J , it sets the number of windings taken into account to reach required numerical accuracy. In the same fashion, $u^2 \equiv \sum_{\mu} (u^{\mu})^2$ renormalizes the bare Josephson energy, $E'_J = E_J \exp(-u^2/2)$ (note that the previously defined term E_J^* appears only in the linearized Hamiltonian used to derive the ansatz, and acts only as a variational parameter).

E_J^* optimisation. The anharmonicity of the cos-shaped potential tends to soften the phase confinement compared to quadratic potential, thus enhancing the zero point phase fluctuations. Having built an ansatz adapted to the specifics of the problem, we can use it as starting point for a variational method. The free parameter is the effective stiffness of the potential E_J^* in the linearized Hamiltonian (S18). We need to compute the energy expectation value of the full Hamiltonian (S17) within the compactified ground state of the linearized Hamiltonian (S18). It is noteworthy that \hat{H} is 2π -periodic, but not gauge invariant. Instead, we make use of $\hat{U} \hat{H}(n_g) \hat{U}^\dagger = \hat{H}(0)$. Using once again the decomposition (S20),

$$\frac{\langle 0_{\mathcal{O}}|\hat{H}|0_{\mathcal{O}}\rangle}{\langle 0_{\mathcal{O}}|0_{\mathcal{O}}\rangle} = \sum_{\mu} \frac{\Omega_{\mu}}{2} - E_J \frac{u^2}{2} - E_J \left(\sum_{w \in \mathbb{Z}} e^{-2(\pi w)^2 v^2 - i2\pi w n_g} \right)^{-1} \sum_{w \in \mathbb{Z}} \left(\frac{(\pi w)^2}{2} + (-1)^w e^{-\frac{u^2}{2}} \right) e^{-2(\pi w)^2 v^2 - i2\pi w n_g}. \quad (\text{S27})$$

The E_J^* dependence is contained in u^2 and v^2 . The full numerical procedure consists, at every step, in a minimization of the expression (S27) over E_J^* , using a fast diagonalization the arrowhead \mathbf{M} matrix (S19) for the new value of E_J^* , and the computation of the two scalars u^2 and v^2 . We then compute the energy expectation value (S27) with a number of terms in the sums over w controlled by v^2 . Since the $w \neq 0$ terms are exponentially suppressed, the sums are rapidly convergent. In practice, we need at most $w \sim 10$ terms when the Josephson energy is close to the breaking point of the method, $E_J/E_c \sim 1$. Crucially, u^2 is independent of the number of modes. Overall, the complexity of the whole procedure is $\mathcal{O}(N_{\text{modes}}^2)$, with N_{modes} the total number of modes in the chain.

PERTURBATION THEORY AT SMALL COUPLING STRENGTH.

One of the transmon-boson model's striking features is the different responses of the junction's phase fluctuations ($\cos \hat{\varphi}$) to coupling strength α , depending of the E_J/E_c regime, as shown by Fig. 3 of the main text. Broadly speaking, the environment damps the phase fluctuations of the dissipative transmon, but enhance those of the dissipative two-level system. As already emphasized, this behavior cast doubt on the two-level description of the strongly interacting transmon. Arguably, while this feature is correctly described by both NRG and compact ansatz, a simple perturbative analysis in α should already be able to discriminate between these two regimes, and pin-point the break down of the two-level approximation.

We employ time-independent perturbation theory at second order, with $(\hat{n}-1/2) \sum_k i g_k (\hat{a}_k^\dagger - \hat{a}_k)$ as the perturbation. We denote $|\psi_n\rangle$ the eigenstates of the bare qubit, E_n their energies. Then,

$$\begin{aligned} \langle \cos \hat{\varphi} \rangle \simeq & \langle 0 | \cos \hat{\varphi} | 0 \rangle + \sum_{\substack{k \\ n \neq 0 \\ m \neq 0}} g_k^2 \frac{\langle \psi_n | \hat{n} | \psi_0 \rangle \langle \psi_0 | \hat{n} | \psi_m \rangle}{(E_0 - E_n - \omega_k)(E_0 - E_m - \omega_k)} \langle \psi_n | \cos \hat{\varphi} | \psi_m \rangle - \sum_{\substack{k \\ n \neq 0}} g_k^2 \frac{|\langle \psi_n | \hat{n} | \psi_0 \rangle|^2}{(E_0 - E_n - \omega_k)^2} \langle \psi_0 | \cos \hat{\varphi} | \psi_0 \rangle \\ & + 2 \sum_{\substack{k,j \\ i \neq 0}} g_k^2 \frac{\langle \psi_0 | \cos \hat{\varphi} | \psi_i \rangle \langle \psi_j | \hat{n} | \psi_0 \rangle \langle \psi_j | \hat{n} | \psi_i \rangle}{(E_0 - E_i)(E_0 - E_j - \omega_k)}. \end{aligned} \quad (\text{S28})$$

This expression takes into account the multi-level nature of the qubit. It can be reduced by restricting the sum on bare qubit levels to the most significant element:

$$\begin{aligned} \langle \cos \hat{\varphi} \rangle \simeq & \langle 0 | \cos \hat{\varphi} | 0 \rangle + \sum_k g_k^2 \frac{|\langle \psi_1 | \hat{n} | \psi_0 \rangle|^2}{(E_0 - E_1 - \omega_k)^2} \langle \psi_1 | \cos \hat{\varphi} | \psi_1 \rangle - \sum_k g_k^2 \frac{|\langle \psi_1 | \hat{n} | \psi_0 \rangle|^2}{(E_0 - E_1 - \omega_k)^2} \langle \psi_0 | \cos \hat{\varphi} | \psi_0 \rangle \\ & + 2 \sum_k g_k^2 \frac{\langle \psi_1 | \hat{n} | \psi_0 \rangle \langle \psi_1 | \hat{n} | \psi_2 \rangle}{(E_0 - E_2)(E_0 - E_1 - \omega_k)} \langle \psi_2 | \cos \hat{\varphi} | \psi_0 \rangle. \end{aligned} \quad (\text{S29})$$

The first and second term correspond to the two-level approximation (in the limit $\alpha \rightarrow 0$). However, the third term adds the contribution from the third qubit level into the mix. Indeed, this term is mostly responsible for the qualitative change between dissipative two-level and dissipative transmon when E_J/E_c is increased, as shown by the Fig. S1.

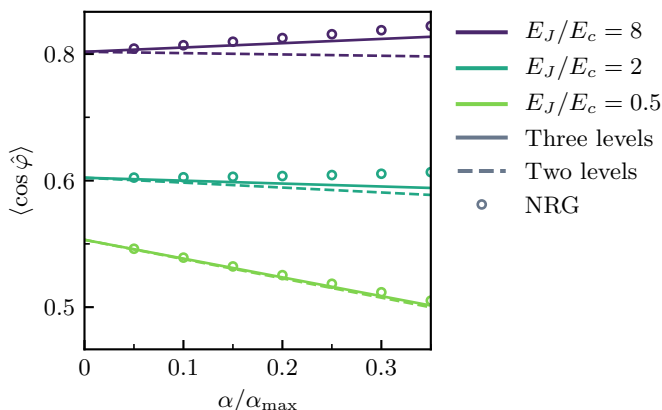


FIG. S1. NRG estimates for phase fluctuations as a function of α (circles), compared to the two and three levels approximation within first order perturbation theory (dashed and solid lines respectively). The two levels approximation (dashed lines) clearly fails in the transmon regime, where the slope changes of sign, while bringing the third level improves the agreement to NRG.